

## **Bivariate statistics of floating offshore wind turbine dynamic response under operational conditions**

Xiaosen Xu<sup>1)</sup>, Oleg Gaidai<sup>2\*)</sup>, Arvid Naess<sup>3)</sup>, Wang Fang<sup>2)</sup>, Yihan Xing<sup>4)</sup>, Junlei Wang<sup>5)</sup>

1) Jiangsu University of Science and Technology, Zhenjiang, China

2) Shanghai Ocean University, China

3) Norwegian University of Science and Technology, Norway

4) University of Stavanger, Norway

5) Guilin University of Electronic Technology, Guilin, China

### **Abstract**

Floating offshore wind turbines (FOWT) belong to the contemporary offshore wind energy industry generating green renewable energy. Accurate prediction of extreme loads and responses during FOWT offshore operation is an important design concern. In this paper, the OpenFAST code was used to analyse offshore wind turbine mooring line tension force and internal bending moment due to environmental hydrodynamic wave loads, acting on a specific FOWT under actual local sea conditions. This paper advocates a computationally efficient Monte Carlo based methodology to study bivariate extreme dynamic response statistics. The bivariate ACER2D (average conditional exceedance rate) method is briefly discussed. The ACER2D method enables accurate estimation of bivariate statistics, utilizing available data efficiently. Large return period two-dimensional probability contours, were obtained using the ACER2D method. Based on the overall performance of the presented method, it is seen that the ACER2D method provides an efficient and accurate prediction of extreme return period contours. More accurate and reliable estimations of extreme responses are significant for the offshore wind industry as it advances the design, manufacturing and deployment of large FOWTs in the coming decade.

The described approach may be well used at the design stage, while defining optimal wind turbine design values that would minimize potential FOWT structural damage due to excessive environmental loadings. Note that the bivariate design point is less conservative than the classic univariate one, therefore this study advocates a design method leading to lower structural production costs.

### **Keywords**

Floating offshore wind turbine (FOWT); Monte Carlo; bivariate distribution; wind energy.

\*) Corresponding author: Oleg Gaidai; email: oleg.gaidai@yahoo.com

## 1. Introduction

Wind energy is an important component of the renewable green energy industrial sector within the expanding offshore energy industry. Offshore wind energy is typically generated by wind farms installed offshore harvesting wind energy and generating green electricity. Offshore wind speeds are on average stronger compared to those onshore, therefore offshore wind energy contribution in terms of electricity supplied, is of industrial importance. Low ocean surface roughness normally leads to higher mean wind speeds. FOWTs are naturally exposed to violent turbulent wind flows and hydrodynamic loads, thus their extreme load capacities are of engineering importance for FOWT design. There are several floating wind farms that are now in the planning stage, and one operated floating wind farm called Hywind Scotland. With the trend that harnessing offshore wind energy moves to the deep water, studying bivariate extreme loads of FOWTs becomes more significant.

There are usually two approaches for obtaining FOWT design loads: (1) simulate rare events **with** that cause high load levels; (2) simulate turbine response under normal environmental conditions and extrapolate structural loads and responses by fitting extreme tail probability distribution (Dimitrov, 2016). Both of the aforementioned procedures for attaining extreme design loads are recommended by the IEC 61400-1 standard (IEC, 2005). This article will discuss the second strategy (b), which is concerned with long-term probability distributions. The latter approach is statistically more precise since it utilizes full statistical distributions, instead of single extreme load/response events. This study thus advocates a methodology that has been already validated for a wide range of offshore marine structures including various vessels and offshore platforms (Gaidai et. al., 2018; Zhang et. al., 2019; Gaidai et. al., 2016; Naess et. al., 2010; Naess et. al., 2009; Naess et. al., 2008; Naess and Moan, 2013). Figure 1 presents an example of a semi-submersible FOWT, similar to the target model analyzed in this paper.



**Figure 1. An example of FOWT in offshore field operation.**

Numerous studies were conducted in the past, aiming at accurate estimation of ultimate loads within the framework of offshore wind turbines design. Fogle et. al. (2008) applied block maxima and global maxima for a wind turbine loads extrapolation. Ernst and Seume (2012) used data from FINO (Research platforms in the North Sea and Baltic Sea) platform to investigate turbulent intensity and extreme loads of a 5 MW wind turbine using a POT (peaks-over-threshold) extrapolation method. Dimitrov (2016) presented four extrapolation techniques applied to FOWT environmental loads. Li et. al. (2015) developed semi-submersible floating wind turbine MATLAB code for dynamic analysis. Graf et al. (2016) studied long-term fatigue loads of a FOWT by using the Monte Carlo method. Aggarwal et al. (2017) studied a spar-type FOWT nonlinear short-term extreme responses. Dimitrov et al. (2018) proposed a procedure for quick assessment of site-specific lifetime fatigue loads by means of surrogate models. Li et. al. (2018) studied effects of numerical simulation length on accumulated FOWT fatigue damage. Zhao and Dong (2021) investigated the long-term extreme response analysis for semi-submersible platform mooring systems and the proposed method was shown to be effective compared with traditional environmental contour methods. Qu et al. (2021) compared short-term extreme response of FOWT using two different blade models and the result revealed that linear beam model would underestimate the extreme load. However, the approaches described above to fit the empirical data to an assumed extreme value distribution do not accurately reflect the inherent properties of the data. This may result in less trustworthy predictions, which is particularly more crucial when predicting extreme values. Extreme values are obtained near the tail of the probability distribution and are thus very sensitive to uncertainties and errors.

This paper aims at efficient use of simulated structural data. For that purpose, the novel bivariate averaged conditional exceedance rate (ACER2D) method has been applied. The available structural load statistics is combined with a matching class of parametric functions for extrapolating the bivariate extreme value distribution tail surface. The ACER2D method does not rely on the generalized extreme value distribution (GEV) assumption, the latter makes the ACER2D method more suitable to analyze actual data sets which are rarely truly asymptotic. The latter inconsistency between pre-assumed asymptotic behavior on actual non-asymptotic data may occasionally lead to errors in long return period design value predictions. A clear engineering design merit of the advocated statistical approach, compared with the example using direct Monte Carlo method, is that far fewer numerical simulations are required to provide comparably accurate extreme value estimates.

## 2. Environmental conditions

It is often difficult to find high quality metocean data with sufficient temporal resolution. The National Oceanic and Atmospheric Administration (NOAA) was used as a data source for this study. The NOAA organization possesses an extensive network of offshore floating data gathering buoys spread over US and international waters. Data from these buoys can be obtained at the US National Data Buoy Center (<https://www.ndbc.noaa.gov/>).

This study therefore used data downloaded from the NOAA website. The 8 years 2010-2017 of available environmental data were selected. Selected buoys readings included five measurement signals: mean wind speed, wave peak-spectral period, significant wave height, wind and wave directions. For this paper only three major measurement signals were selected, the latter however is not a limitation of the suggested approach. Requirements for a wave direction measurement led to a selection of 23 offshore sites. Figure 2 indicates names and locations of selected from the NOAA database.

The wind-wave data was collected and processed by different device sensors. The wind speed and direction data were averaged over 8 min period and recorded hourly. The significant wave height was defined as the average height of the highest one-third of waves over a 20 min period, recorded hourly. Peak-spectral period corresponded to the wave period with the greatest wave energy over the same 20 min period. Wave direction was the direction from which the dominant period waves arrived.

National Data Buoy Center Station Cape Elizabeth was selected for the present study. The measurement buoy was located about 45 nautical miles Northwest of Aberdeen, Washington; near the continental shelf edge at the water depth about 125 m. Figure 2 presents various US National Data Buoy Centre stations along with Cape Elizabeth location indicated in red (Stewart et. al., 2016). Joint wind-wave directional statistics for the above-mentioned location was assessed based on the in situ metocean hourly historical data measured during 2010-2017 years.



**Figure 2. US National Data Buoy Center stations. Cape Elizabeth is marked in red.**

Figure 3 presents the Monte Carlo based long term statistical analysis flow chart utilized in this paper. Note that "sea state" implies a full set of recorded environmental conditions, including wind direction and speed.

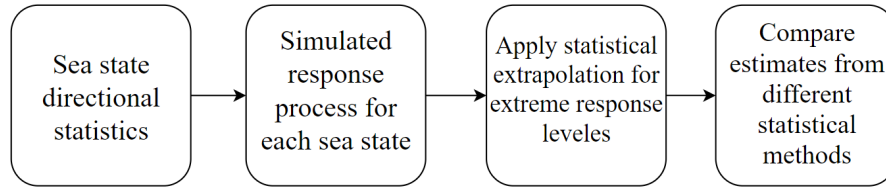


**Figure 3. Flow chart for long term statistical analysis.**

Data post-processing then proceeded with extrapolating of the wind speed to the FOWT hub height of 90 m. Cape Elizabeth's anemometers were installed at a height of 5 meters above sea level. Most engineering techniques use either power law or log law wind shear equations to extrapolate, see Eqs (1) and (2), respectively:

$$U(z) = U(z_r) \left( \frac{z}{z_r} \right)^\alpha \quad (1)$$

$$U(z) = U(z_r) \frac{\ln(z) - \ln(z_0)}{\ln(z_r) - \ln(z_0)} \quad (2)$$

with  $U(z)$ ,  $U(z_r)$  being wind speeds at height  $z$  and the reference wind speed at height  $z_r$  respectively.  $z_0$  being the surface roughness length and  $\alpha$  being the power law constant. In this paper the power law given by Eq. (1) has been equal  $\alpha=0.14$ , see Xu et. al. (2020) . Following conditionalities were used, according design standards, see e.g. Xu et. al. (2020):

- Wind speed  $U$
- Significant wave height  $H_s$
- Peak-spectral period  $T_p$

In this paper a scatter diagram approach was utilized, the measured buoy data was post-processed into an empirical three dimensional joint distribution, without any simplifications and assumptions. A three-

dimensional scatter map was generated by directly estimating the empirical joint probability density function (PDF)  $p(U, H_s, T_p)$  from the available observed metocean data. Due to the fact that the wind/wave misalignment is not included in the OpenFAST simulation, only the latter three-dimensional probability space  $(U, H_s, T_p)$  was used. It has to be noted that the described approach is well suitable for higher dimensional scatter diagrams. Figure 4 on the left presents: wind speed versus significant wave height correlation pattern; on the right:  $(H_s, T_p)$  contour plot,  $p(H_s, T_p) = \int p(U, H_s, T_p) dU$ .

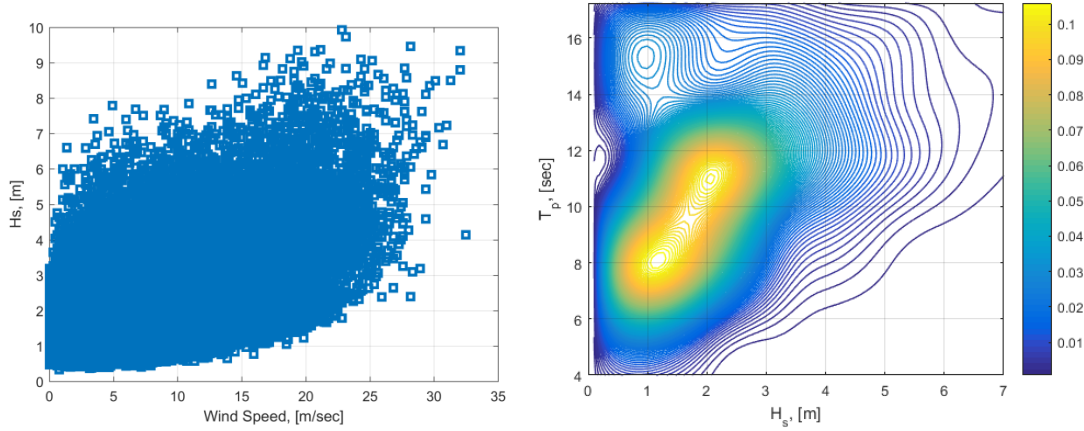


**Figure 4. Left: In situ wind speed vs significant wave height correlation pattern; Right:  $(H_s, T_p)$  contour plot of the joint probability density  $p(H_s, T_p) = \int p(U, H_s, T_p) dU$ .**

The advocated technique is a direct Monte Carlo long term simulation approach, having the advantage of not incorporating various assumptions and simplifications, like e.g. Stewart et. al. (2016), where the wind speed was assumed to be an independent parameter (typical in various FOWT engineering applications). Note that Figure 4 on the left, exhibits certain correlation between wind speed  $U$  and significant wave height  $H_s$ . Thus, it is not always accurate to pre-assume wind speed as an independent parameter.

For this study, a total 12 different wind speed bins were selected, ranging from 3 to 25 m/sec. For each wind speed bin ( $U$ ), about 30 corresponding sea states  $(H_s, T_p)$  with different probabilities were selected for numerical simulation. In this paper, the scatter diagram of the three dimensional probability distribution  $p(U, H_s, T_p)$  was taken into account within the framework of Monte Carlo simulation. For more details on how the bivariate ACER2D functions correspond to different short term wind-sea states and further combined into one long term ACER2D function, see Gaidai et al. (2016), Gaidai et al. (2017), Gaidai et al. (2018).

Note that this study has relied on the NOAA buoy measured data, with subsequent application of a scatter diagram approach to obtain the empirical multi-dimensional probability density function (PDF). This study did not accommodate satellite data.

### 3. Model description in brief

The DeepCwind semi-submersible supporting platform, namely OC5 semi-submersible floating system (Robertson et. al., 2016) has been chosen as the target model for this study. The model of the semi-submersible platform is shown in Figure 5, and it contains one main column and three outer offset columns. There are heave plates (base columns) attached to the bottom in order to reduce large heave motions.



**Figure5. 1/50 scale model of the DeepCwind semi-submersible platform.**

Table 1 presents the main dimensions of the full scale semi-submersible platform.

**Table 1. Main dimensions of the semi-submersible platform.**

Item	Value
Platform draft	20.0 m
Spacing between offset columns	50.0 m
Length of upper columns	26.0 m
Length of base columns	6.0 m
Diameter of central column	6.5 m
Diameter of offset (upper) columns	12.0 m
Diameter of base columns	24.0 m

The NREL 5-MW baseline wind turbine is placed on top of the OC 5 semi-submersible platform. The diameter of the three-bladed rotor is 126 m, while the hub height of the cylindrical tower is 90 m. The 5-MW baseline wind turbine's parameters are summarized in Table 2.

**Table 2. Summary properties of 5-MW baseline wind turbines.**

Item	Value
Rotor orientation	Upwind, 3 blades
Cut-in/Rated/Cut-out wind speed	3 m/s, 11.4 m/s, 25 m/s
Rotor mass	110,000 kg
Nacelle mass	240,000 kg
Tower mass	347,460 kg
Hub height	90 m

OpenFAST and AeroDyn account for applied aerodynamic and gravitational loads, allowing for accurate numerical modeling of the wind turbine structural dynamics. Various advanced corrections, including tip loss, hub loss, skewed inflow and dynamic stall corrections, are included in the BEM method. The OpenFAST software includes a variety of mechanical effects such as e.g. elasticity of the rotor tower, along with the elastic coupling between their motions and the motions of the support platform as well as dynamic coupling between the support platform motions and the wind turbine motions. OpenFAST is based on a combined modal and multibody structural dynamics formulation (Jonkman et al., 2005).

Numerical simulations for the current study were run with a sufficient number of degrees-of-freedom (DOFs), including OpenFAST two flap wise and one edgewise mode DOFs per blade, one drivetrain torsion DOF, one variable generator-speed DOF, one nacelle yaw DOF, two fore-aft and two side-to-side tower mode DOFs, as well as floating system DOFs, namely three translational (surge, sway, and heave) and three rotational (roll, pitch, and yaw) DOFs of the platform (Jonkman et al., 2007).

#### 4. Dynamic analysis of wind turbine simulations

To model various coupled system reactions in this investigation, the aero-hydro-servo-elastic simulation code OpenFAST (Jonkman et al., 2005) was employed. TurbSim (Jonkman, 2009) generates stochastic wind fields on a 31×31 square grid with a 145 m width. AeroDyn, an OpenFAST code module, was capable of modeling the aerodynamics of baseline wind turbines using the blade element momentum approach while taking into account rotor-wake effects and dynamic stall. The structural dynamic responses in the time domain are determined by solving the rigid-flexible coupled system's equations of motion, which are derived using Kane's technique. Hydrodynamic loads were modeled using the OpenFAST HydroDyn (Jonkman et al., 2014) module, which integrates both Morison's equation and potential flow theory for large-diameter structures. Potential flow theory is used to predict hydrodynamic coefficients such as additional mass and potential damping coefficients in the frequency domain. To account for viscous drag forces operating on FOWT, Morison's equation incorporated a drag force component. Second-order wave forces have also been included into the OpenFAST numerical simulation (Bayati et al., 2014). NREL 5MW semi-submersible FWTs use MoorDyn mooring module that is based on lumped mass theory. The control system used in the 5MW FOWT is implemented by ROSCO.

According to IEC-61400-1 from the International Electro technical Commission (2005), at least 15 short term simulations of 10 minute duration were needed for ultimate loads extrapolation, with a target return time of 50 years under normal production circumstances. Based on IEC-61400-3 from the International Electro-technical Commission (2009), Design Load Case (DLC) 1.1, for the current study the total of 2550 times 10 min short term random cases have been numerically simulated, with cut-in wind speed 3 m/s and cut-out wind speed 25 m/s. Speed scatter diagram bin size was set to 2 m/s. Each simulation was set to a total duration of 800 seconds, with the first 200 seconds being excluded from post processing owing to initial temporary effects. Three wind speed (7m/s, 11m/s and 15m/s, also denoted as below-rated, rated and over-rated cases) are selected as the sample wind speeds for sample plotting. Figure 6 presents sample time series plots of

platform pitch, tower base fore-aft bending moment (TwrBsMyt), blade root out-of-plane bending moment (RootMyc) and mooring line tension. The mean value of the tower base fore-aft bending moment is non-zero because of the wind turbine thrust force and is proportional to the wind turbine thrust force. It indicates that ultimate structural loads are more likely to reach a certain extreme level when subject to large wind forces. Besides, the obvious fluctuating component is observed, and therefore the ultimate structural loads are determined by both aerodynamic and hydrodynamic excitation.

Extensive experimental work has been undertaken on the OC4 and OC5 projects in order to provide experimental data that can be used to validate floating offshore wind turbine modeling tools (Coulling et al. 2013; Benitz et al. et al., 2015). The average error with respect to experimental results across OC5 OpenFAST numerical results was about 10% under-prediction of the tower top ultimate shear load; about 14% under-prediction for the tower-base load; and approximately 20% under-prediction of the upwind mooring tension for wave-only cases (Robertson et. al., 2017). The experimental validation results give the authors confidence in selecting OpenFAST as a numerical simulation tool for this research.

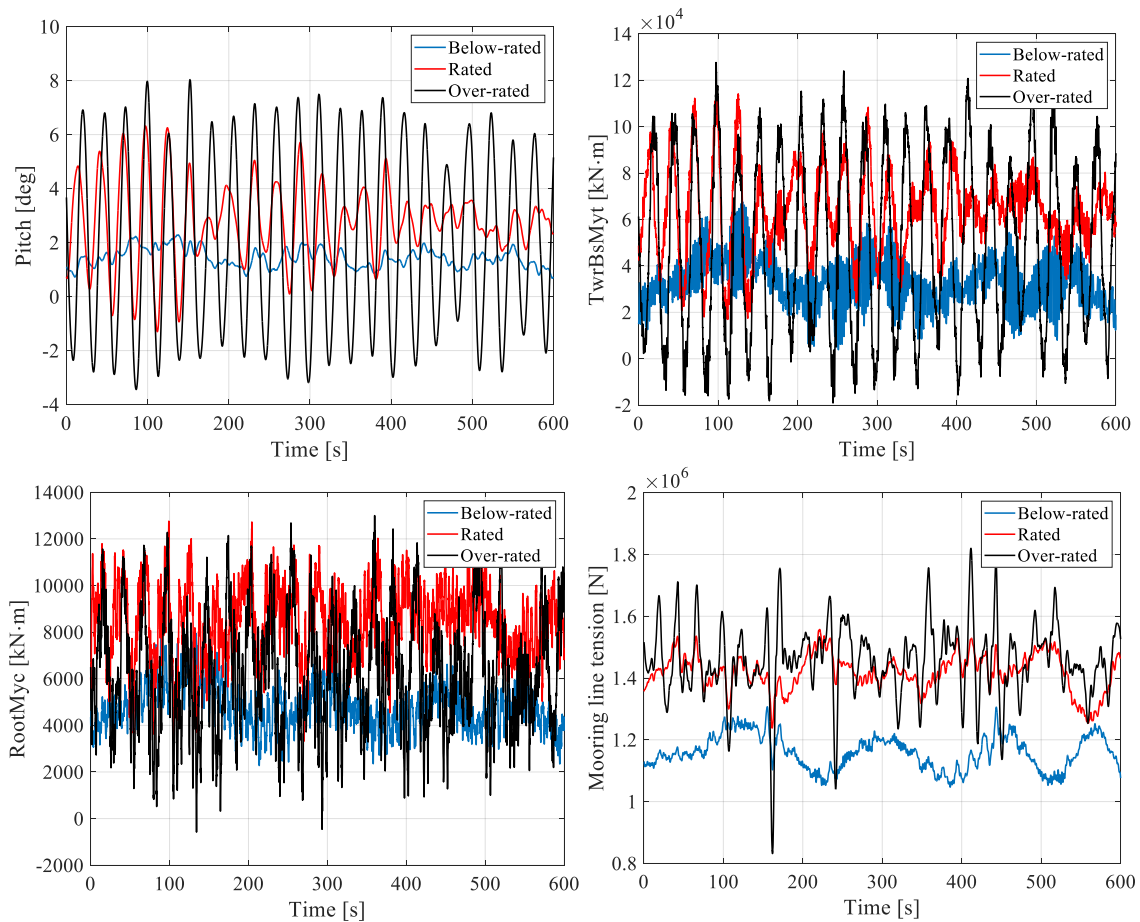
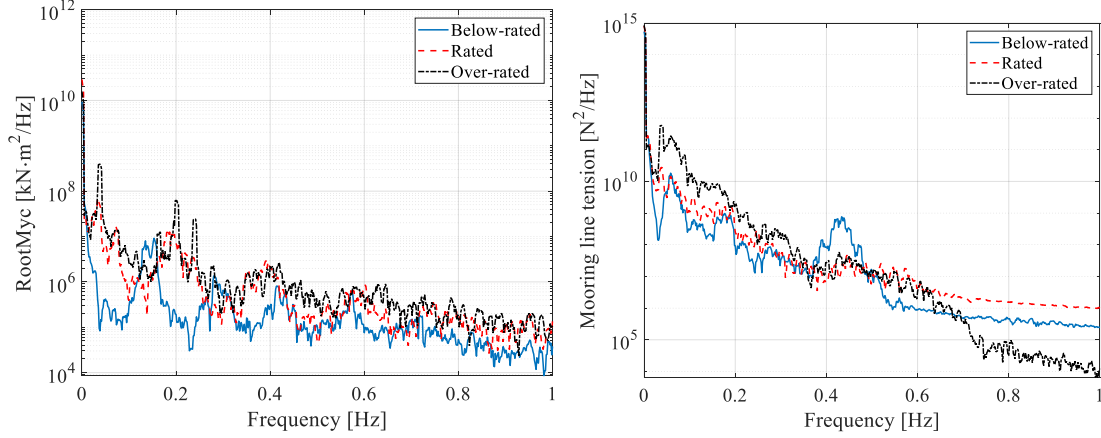


Figure 6 Sample time series when  $U_{hub} = 7, 11, 15\text{m/s}$





**Figure 7 PSD of the blade root out-of-plane bending moment and mooring line tension**

Fig. 7 presents the corresponding power spectral density (PSD) of the blade root bending moment out-of-plane and mooring line tension. It can be seen from Fig. 7 that there is a characteristic period around 5 sec (frequency 0.2 Hz) (**Incorrect, dt=0.05s**) with pronounced narrow band nature. Since simulated time series consisted of discrete temporal data points with constant time increment  $\Delta t = 0.05$  sec ( **$\Delta t = 0.2$  is FPSO, not FOWT**), bending moment PSD from Fig. 7 suggests blocking (comprising) of time series into consequent  $T = k\Delta t = 5$  seconds maxima, with  $k = 25$  being ACER proper conditioning level. The latter T seconds blocked (comprised) simulated maxima constitute the new blade root bending moment time series, that has been used further in this paper for statistical analysis.

## 5. The ACER2D method - statistical approach

The 2D (bivariate) Average Conditional Exceedance Rate, or briefly ACER2D, method has been applied to analyse offshore wind turbine blade root bending moment and mooring line tension force due to environmental hydrodynamic wave loads. It should be noted that both the above mentioned stochastic response processes (blade root bending moment and mooring line tension) are time synchronous, the latter is certainly beneficial for coupling effects and bivariate statistics study. A brief introduction of the bivariate ACER2D method is outlined below, for more details see Gaidai et al. (2016), Gaidai et al. (2017), Gaidai et al. (2018), Naess et al (2008), Naess et al (2009a), Naess et al (2009b), Naess et al (2010).

This paper studies the bivariate stochastic process  $Z(t) = (X(t), Y(t))$ , having two scalar component processes  $X(t)$  and  $Y(t)$  simulated synchronously, over a time span  $(0, T)$ . The bivariate data points  $(X_1, Y_1), \dots, (X_N, Y_N)$  correspond to equidistant time instants  $t_1, \dots, t_N$ .

The CDF (joint cumulative distribution function)  $P(\xi, \eta) := \text{Prob}(\hat{X}_N \leq \xi, \hat{Y}_N \leq \eta)$  of the maxima vector  $(\hat{X}_N, \hat{Y}_N)$ , with  $\hat{X}_N = \max\{X_j; j = 1, \dots, N\}$ , and  $\hat{Y}_N = \max\{Y_j; j = 1, \dots, N\}$  is introduced. In this paper  $\xi$  and  $\eta$  are blade root bending moment and mooring line tension force, respectively.

Next, the non-exceedance event is introduced:  $\mathcal{C}_{kj}(\xi, \eta) := \{X_{j-1} \leq \xi, Y_{j-1} \leq \eta, \dots, X_{j-k+1} \leq \xi, Y_{j-k+1} \leq \eta\}$  for  $1 \leq k \leq j \leq N + 1$ . Based on the definition of the CDF  $P(\xi, \eta)$ ,

$$\begin{aligned}
 P(\xi, \eta) &= \text{Prob}(\mathcal{C}_{N+1, N+1}(\xi, \eta)) \\
 &= \text{Prob}(X_N \leq \xi, Y_N \leq \eta \mid \mathcal{C}_{NN}(\xi, \eta)) \cdot \text{Prob}(\mathcal{C}_{NN}(\xi, \eta)) \\
 &= \prod_{j=2}^N \text{Prob}(X_j \leq \xi, Y_j \leq \eta \mid \mathcal{C}_{jj}(\xi, \eta)) \cdot \text{Prob}(\mathcal{C}_{22}(\xi, \eta))
 \end{aligned} \tag{4}$$

The CDF  $P(\xi, \eta)$  can expressed as (see **Error! Reference source not found.-Error! Reference source not found.**)

$$P(\xi, \eta) \approx \exp\left\{-\sum_{j=k}^N \left(\alpha_{kj}(\xi; \eta) + \beta_{kj}(\eta; \xi) - \gamma_{kj}(\xi, \eta)\right)\right\} \quad (5)$$

for a suitably large conditioning level parameter  $k$ , and large  $\xi$  and  $\eta$  with  $\alpha_{kj}(\xi; \eta) := \text{Prob}(X_j > \xi \mid \mathcal{C}_{kj}(\xi, \eta))$ ,  $\beta_{kj}(\eta; \xi) := \text{Prob}(Y_j > \eta \mid \mathcal{C}_{kj}(\xi, \eta))$ ,  $\gamma_{kj}(\xi, \eta) := \text{Prob}(X_j > \xi, Y_j > \eta \mid \mathcal{C}_{kj}(\xi, \eta))$ . Next, the  $k$ -th order bivariate average conditional exceedance rate (ACER2D) functions are introduced

$$\mathcal{E}_k(\xi, \eta) = \frac{1}{N - k + 1} \sum_{j=k}^N \left(\alpha_{kj}(\xi; \eta) + \beta_{kj}(\eta; \xi) - \gamma_{kj}(\xi, \eta)\right) \quad (6)$$

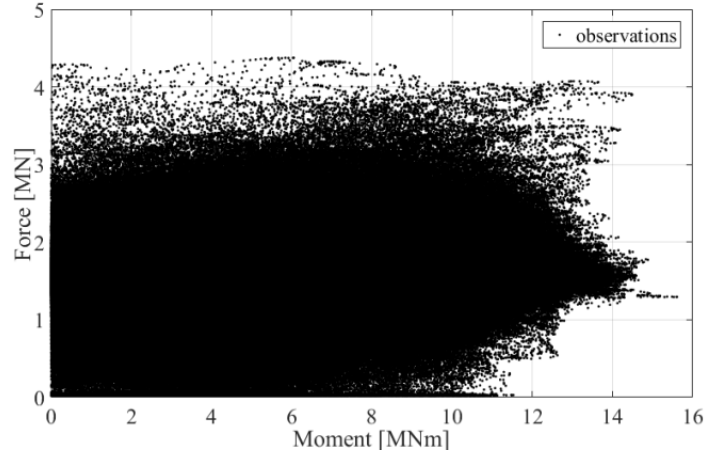
for  $k = 1, 2, \dots$ ; when  $N \gg k$ ,

$$P(\xi, \eta) \approx \exp\{- (N - k + 1)\mathcal{E}_k(\xi, \eta)\}; \text{ for large } \xi \text{ and } \eta. \quad (7)$$

From Eq. (7), it is seen that accurate estimate of the bivariate CDF  $P(\xi, \eta)$  relies on the equally accurate estimation of ACER2D functions  $\mathcal{E}_k$ .

## 6. Extreme bivariate load analysis

This section provides the bivariate statistical results using the ACER2D method, for the dynamic loading time series, obtained from the aero-hydro-servo-elastic simulation OpenFAST code simulation.



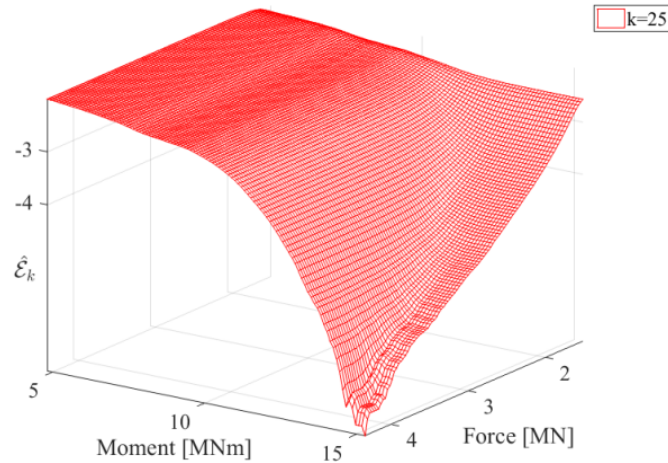


**Figure 8 Up: moment- force correlation pattern. Down: ACER2D  $\hat{\mathcal{E}}_k$  function plotted on a decimal logarithmic scale, with conditioning level  $k = 25$ .**

Figure 8 on the right presents the bivariate ACER2D functions  $\hat{\mathcal{E}}_k$  empirically calculated for conditioning level  $k = 25$  on a decimal logarithmic scale.

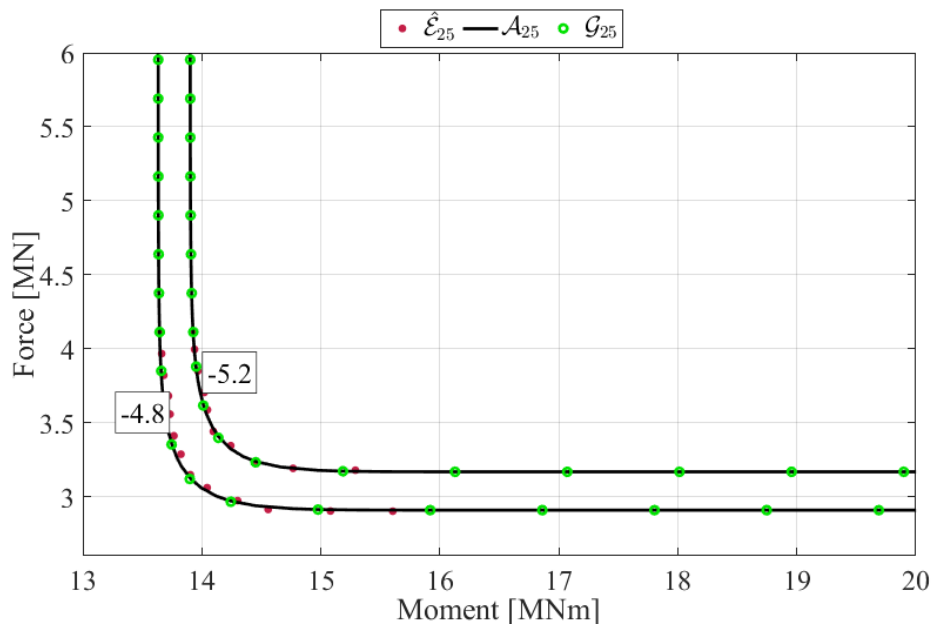


**Figure 9 Empirically estimated  $\hat{\mathcal{E}}_{25}$  surface ( $\bullet$ ) contour plot, along with optimized Gumbel logistic  $\mathcal{G}_{25}$  ( $\circ$ ) and optimized Asymmetric logistic  $\mathcal{A}_{25}$  ( $-$ ) surfaces. Negative labeling numbers correspond to probability levels on decimal logarithmic scale.**

Figures 9, 10 show optimized Asymmetric logistic (AL)  $\mathcal{A}_k(\xi, \eta)$  and optimized Gumbel logistic (GL)  $\mathcal{G}_k$  models contour lines, optimally matched to the empirical bivariate ACER2D function  $\hat{\mathcal{E}}_k$ ,  $k = 25$ , see Gaidai et al. (2016), Gaidai et al. (2017), Gaidai et al. (2018) for GL and AL definitions in terms of the marginal ACER1D functions. The optimized models  $\mathcal{G}_{25}$  and  $\mathcal{A}_{25}$  exhibit smooth contours well matching ACER2D empirical contours. The latter models are therefore suitable for bivariate response extreme value distributions for the applications in this paper. Figure 9 shows good agreement between optimized AL and GL surfaces and empirical bivariate ACER2D surface. It is obvious that correlation between wind turbine blade root bending moment and mooring line tension force is not pronounced, judging from the shape of the bivariate contour lines. The lowest probabilities in Figure 9 correspond to the value  $N^{-1}$  where  $N$  is the number of

equidistant time points in the corresponding time series, see Eqs. (4) - (7) in the previous section.

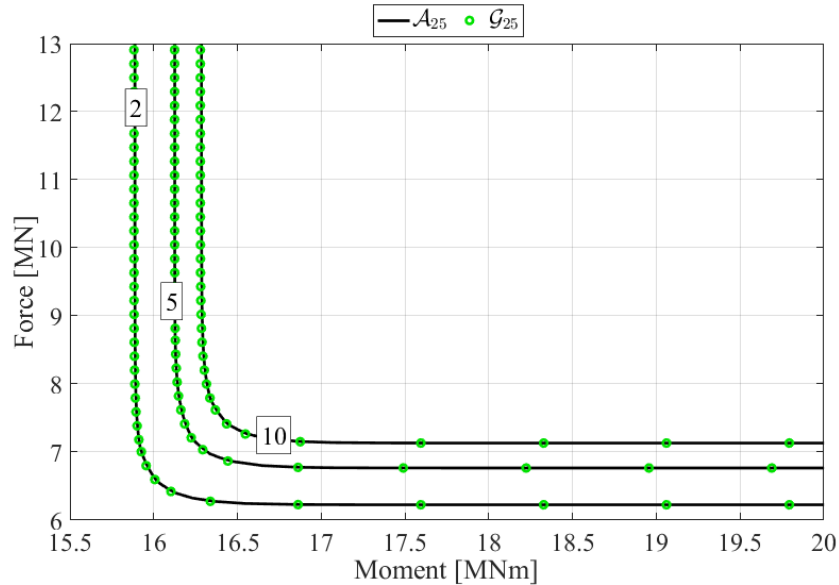


**Figure 10 Predicted return period contours for optimized Gumbel logistic  $\mathcal{G}_{25}$  (•) and optimized Asymmetric logistic  $\mathcal{A}_{25}$  (—) surfaces. Boxes indicate return periods in years.**

Figure 10 presents predicted return period contours for optimized Gumbel logistic  $\mathcal{G}_{25}$  and optimised Asymmetric logistic  $\mathcal{A}_{25}$  surfaces, with return periods indicated in years. Clearly, both Gumbel logistic and Asymmetric logistic models are in a very good match. It is seen that correlation between tension force and bending moment is influencing the shape of the bivariate contour lines. Bivariate contour lines corresponding to large return periods, e.g. 10 years return period, are important **safe** engineering design components. Therefore, the above mentioned results are of practical engineering importance, especially given the advantage of the bivariate statistical analysis over the classical univariate one.

## 7. Conclusions

The offshore wind turbine mooring line tension force and internal bending moment due to environmental hydrodynamic wave loads were studied. The bivariate ACER2D method was briefly described and applied to account for the coupled load effects, namely dynamic moment and force simulated synchronously in time. Bivariate extreme value distribution low probabilities (or equivalently high quantiles) contours were estimated by adopting various bivariate copula models.

Regarding safety and reliability of FOWT operations, the multivariate analysis is obviously a more proper approach, than classic univariate approach. The presented technique has following advantages:

- Unlike IFORM/ SORM, ACER2D method does not simplify model non-linearities.
- Various kinds of coupled data can be studied: either measured or numerically simulated.
- Clustering effects can be accounted for.
- Unlike various methods based on asymptotic assumptions (e.g. Gumbel, Pareto, POT, Weibull) the ACER2D method provides an accurate estimate of the exact bivariate extreme value distribution without directly involving asymptotic assumptions.
- ACER2D method may provide an efficient way of identifying appropriate bivariate copula models for practical design.

## 8. Acknowledgement

This study is funded by National Natural Science Foundation of China [Grant No. 5210110117].

## 9. References

- Aggarwal N, Manikandan R, Saha N. 2017. "Nonlinear short term extreme response of spar type floating offshore wind turbines". *Ocean Eng.* 130, pp. 199–209.
- Bayati, I., Jonkman, J., Robertson, A., Platt, A. (2014). "The effects of second-order hydrodynamics on a semi-submersible floating offshore wind turbine." In *Journal of Physics: Conference Series* (Vol. 524, No. 1, p. 012094). IOP Publishing.
- Chen, X., Jiang, Z., Li, Q., & Li, Y. (2019). Effect of wind turbulence on extreme load analysis of an offshore wind turbine. In *International Conference on Offshore Mechanics and Arctic Engineering* (Vol. 58769, p. V001T01A038). American Society of Mechanical Engineers.
- Benitz, M. A., Schmidt, D. P., Lackner, M. A., Stewart, G. M., Jonkman, J., Robertson, A. (2015). "Validation of hydrodynamic load models using CFD for the OC4-DeepCwind semi-submersible." National Renewable Energy Lab.(NREL), Golden, CO (United States).
- Coulling, A. J., Goupee, A. J., Robertson, A. N., Jonkman, J. M., Dagher, H. J. (2013). "Validation of a FAST semi-submersible floating wind turbine numerical model with DeepCwind test data." *Journal of Renewable and Sustainable Energy*, 5(2), 023116.
- Dimitrov, N. (2016). Comparative analysis of methods for modelling the short-term probability distribution of extreme wind turbine loads. *Wind Energy*, 19(4), 717-737.
- Dimitrov, N., Kelly, M., Vignaroli, A., & Berg, J. (2018). From wind to loads: wind turbine site-specific load estimation using databases with high-fidelity load simulations. *Wind Energ. Sci. Discuss.*, 375, 767-790.
- Ernst, B., Seume, J. R. (2012). Investigation of site-specific wind field parameters and their effect on loads of offshore wind turbines. *Energies*, 5(10), 3835-3855.
- Fogle, J., Agarwal, P., Manuel, L. (2008). Towards an improved understanding of statistical extrapolation for wind turbine extreme loads. *Wind Energy: An International Journal for Progress and Applications in Wind Power Conversion Technology*, 11(6), 613-635.
- Gaidai, O., Storhaug, G., & Naess, A. (2016). Extreme value statistics of large container ship roll. *Journal of Ship Research*, 60(2), 92-100.
- Gaidai, O., Ji, C., Kalogeri, C., Gao, J. (2017). SEM-REV energy site extreme wave prediction, *Renewable Energy*, Vol 101, pp. 894-899.
- Gaidai, O., Cheng, Y., Xu, X., & Su, Y. (2018). Long-term offshore Bohai bay Jacket strength assessment based on satellite wave data. *Ships and Offshore Structures*, 13(6), 657-665.
- Graf, P. A., Stewart, G., Lackner, M., Dykes, K., & Veers, P. (2016). High-throughput computation and the applicability of Monte Carlo integration in fatigue load estimation of floating offshore wind turbines. *Wind Energy*, 19(5), 861-872.
- International Electrotechnical Commission. (2005). IEC 61400-1: Wind turbines part 1: Design requirements. International Electrotechnical Commission, 177.
- International Electrotechnical Commission. (2009). IEC 61400-3 Wind Turbines Part3: Design Requirements for Offshore Wind Turbines. International Electrotechnical Commission: Geneva, Switzerland.
- Jian, Z., Gaidai, O., & Gao, J. (2018). Bivariate Extreme Value Statistics of Offshore Jacket Support Stresses in Bohai Bay. *Journal of Offshore Mechanics and Arctic Engineering*, 140(4), 041305.

- Jonkman, J. M., Buhl Jr, M. L. (2005). "FAST user's guide." National Renewable Energy Laboratory, Golden, CO, Technical Report No. NREL/EL-500-38230.
- Jonkman, J. M., Buhl Jr, M. L. (2007), "Loads Analysis of a Floating Offshore Wind Turbine Using Fully Coupled Simulation" WindPower 2007 Conference & Exhibition.
- Jonkman, B. J. (2009). "TurbSim user's guide: Version 1.50 (No. NREL/TP-500-46198)." National Renewable Energy Lab. (NREL), Golden, CO (United States).
- Jonkman, J. M., Robertson, A., Hayman, G. J. (2014). "HydroDyn user's guide and theory manual." National Renewable Energy Laboratory.
- Li, L., Hu, Z., Wang, J., Ma, Y. (2015). Development and validation of an aero-hydro simulation code for offshore floating wind turbine. *J. Ocean Wind Energy*, 2(1), 1-11.
- Li, H., Hu, Z., Wang, J., Meng, X. (2018). "Short-term fatigue analysis for tower base of a spar-type wind turbine under stochastic wind-wave loads." *International Journal of Naval Architecture and Ocean Engineering*, 10(1), 9-20.
- Naess, A., & Gaidai, O. (2008). Monte Carlo methods for estimating the extreme response of dynamical systems. *Journal of Engineering Mechanics*, 134(8), 628-636.
- Næss, A., & Gaidai, O. (2009a). Estimation of extreme values from sampled time series. *Structural Safety*, 31(4), 325-334.
- Naess, A., Gaidai, O., & Batsevych, O. (2010). Prediction of extreme response statistics of narrow-band random vibrations. *Journal of Engineering Mechanics*, 136(3), 290-298.
- Naess, A., Stansberg, C. T., Gaidai, O., & Baarholm, R. J. (2009b). Statistics of extreme events in airgap measurements. *Journal of Offshore Mechanics and Arctic Engineering*, 131(4), 041107.
- Naess, A., & Moan, T. (2013). *Stochastic dynamics of marine structures*. Cambridge University Press.
- Robertson, A., Jonkman, J., Wendt, F., Goupee, A., & Dagher, H. (2016). Definition of the OC5 DeepCwind semisubmersible floating system. Technical report.
- Robertson, A. N., Wendt, F., Jonkman, J. M., Popko, W., Dagher, H., Gueydon, S., ... & Soares, C. G. (2017). OC5 project phase II: validation of global loads of the DeepCwind floating semisubmersible wind turbine. *Energy Procedia*, 137, 38-57.
- Stewart, G. M., Robertson, A., Jonkman, J., & Lackner, M. A. (2016). The creation of a comprehensive metocean data set for offshore wind turbine simulations. *Wind Energy*, 19(6), 1151-1159.
- Naess, A., Gaidai, O., Teigen, P. (2007a), Extreme response prediction for nonlinear floating offshore structures by Monte Carlo simulation. *Applied Ocean Research* 2007, Vol. 29.(4) p. 221-230.
- Naess, A., Gaidai, O., Teigen, P. (2007b), Simulation based estimation of extreme response of floating offshore structures. I: Proceedings of the 26th International Conference on Offshore Mechanics and Arctic Engineering. ASME Press, ISBN 0791837998.
- Qu, X., Li, Y., Tang, Y., Chai, W., & Gao, Z. (2020). Comparative study of short-term extreme responses and fatigue damages of a floating wind turbine using two different blade models. *Applied Ocean Research*, 97, 102088.
- Teigen, P., Gaidai, O., Naess, A., (2006), Springing Response Statistics of Tethered Platforms in Random Waves. Proceedings 25th International Conference on Offshore Mechanics and Arctic Engineering. ASME Press, ISBN 0791837777.
- Xu, X., Gaidai, O., Naess, A., Sahoo, P., (2020), Extreme loads analysis of a site-specific semi-submersible type wind turbine, Ships and Offshore structures, DOI: 10.1080/17445302.2020.1733315.
- Zhao, Y., Dong, S. (2021). Long-term extreme response analysis for semi-submersible platform mooring

systems. Proceedings of the Institution of Mechanical Engineers, Part M: Journal of Engineering for the Maritime Environment, 235(2), 463-479.